

# Mitigating Biases with Diverse Ensembles and Diffusion Models

Luca Scimeca<sup>1</sup>, Alexander Rubinstein<sup>2</sup>, Damien Teney<sup>3</sup>,  
Seong Joon Oh<sup>2</sup>, Armand Mihai Nicolicioiu<sup>3</sup>, and Yoshua Bengio<sup>1,4</sup>

<sup>1</sup> Mila - Quebec AI Institute and Université de Montréal, Quebec

<sup>2</sup> Eberhard-Karls-Universität Tübingen, Germany

<sup>3</sup> Idiap Research Institute, Switzerland

<sup>4</sup> CIFAR Senior Fellow

**Abstract.** Spurious correlations in the data, where multiple cues are predictive of the target labels, often lead to a phenomenon known as shortcut learning, where a model relies on erroneous, easy-to-learn cues while ignoring reliable ones. In this work, we propose an ensemble diversification framework exploiting Diffusion Probabilistic Models (DPMs) to mitigate this form of bias. We show that at particular training intervals, DPMs can generate images with novel feature combinations, even when trained on samples displaying correlated input features. We leverage this crucial property to generate synthetic counterfactuals to increase model diversity via ensemble disagreement. We show that DPM-guided diversification is sufficient to remove dependence on primary shortcut cues, without a need for additional supervised signals. We further empirically quantify its efficacy on several diversification objectives, and finally show improved generalization and diversification performance on par with prior work that relies on auxiliary data collection.

**Keywords:** Bias Mitigation · Ensemble Diversity · Diffusion Probabilistic Models

## 1 Introduction

Deep Neural Networks (DNNs) have achieved unparalleled success in countless tasks across diverse domains. However, they are not devoid of pitfalls. One such downside manifests in the form of shortcut learning, a phenomenon whereby models latch onto simple, non-essential cues that are spuriously correlated with target labels in the training data [5, 28, 30]. Often engendered by the under-specification present in data, this simplicity bias often presents easy and viable *shortcuts* to performing accurate prediction at training time, regardless of a model’s alignment to the downstream task. For instance, previous work has found models to incorrectly rely on background signals for object prediction [3, 39], or to rely on non-clinically relevant metal tokens to predict patient conditions from X-Ray images [42]. The phenomenon of shortcut learning has often been found to lead to significant drops in generalization performance [1, 14, 19, 34, 42].

Leveraging shortcut cues can also be harmful when deploying models in sensitive settings. For example, shortcuts can lead to the reinforcement of harmful biases when they endorse the use of sensitive attributes such as gender or skin color [28, 35, 40].

Addressing the simplicity bias in machine learning models has been a focus of extensive research. Numerous studies have aimed to encourage models to use a broader and more diversified set of predictive cues, especially when dealing with training data that lacks explicit shortcut cue labels. A variety of these methods have been input-centric, designed to drive models to focus on different areas of the input space [21, 33], while others have focused on diversification strategies that rely on auxiliary data for *prediction disagreement* [13, 23]. The latter approach, in particular, has been instrumental in developing functionally diverse models that exhibit robustness to shortcut biases, albeit limited by their required access to expensive auxiliary data.

The primary objective of this work is to mitigate shortcut learning tendencies, particularly when they result in strong, unwarranted biases, access to additional data is expensive, and different features may rely on similar areas of the input space. To achieve this objective, we propose an ensemble framework relying on unlabelled *ood* data for diversification. To overcome the challenges of the past, we aim to synthetically generate the data for model disagreement, and thus avoid the impracticality of *ood* data collection. We posit that the synthetic data should: first, lie in the manifold of the data of interest; and second, be at least in part free of the same shortcuts as the original training data. We leverage Diffusion Probabilistic Models (DPMs) to generate synthetic data for ensemble disagreement.

Although the in-depth study of the generalization properties of diffusion sampling mechanisms is beyond the scope of this paper, we make the crucial observation that even in the presence of correlated features in the data, appropriately trained DPMs can be used to generate synthetic counterfactuals that break the shortcut signals present at training time. We show that this important characteristic arises at specific training intervals, and that it can be leveraged for shortcut cue mitigation. We hypothesize that diversification, and shortcut mitigation, can be achieved via ensemble disagreement on these DPM-generated samples, providing models with an opportunity to break the spurious correlations encouraged during training. Remarkably, without a need to control for the diversity in our synthetic samples, our experiments confirm that the extent and quality of our diffusion-guided ensemble diversification is on par with existing methods that rely on additional data.

Our contributions are three-fold:

1. We show that DPMs can generate feature compositions beyond data exhibiting correlated input features.
2. We demonstrate that ensemble disagreement is sufficient for shortcut cue mitigation.
3. We show that counterfactuals from appropriately trained DPMs can be used to achieve state-of-the-art diversification and shortcut bias mitigation.

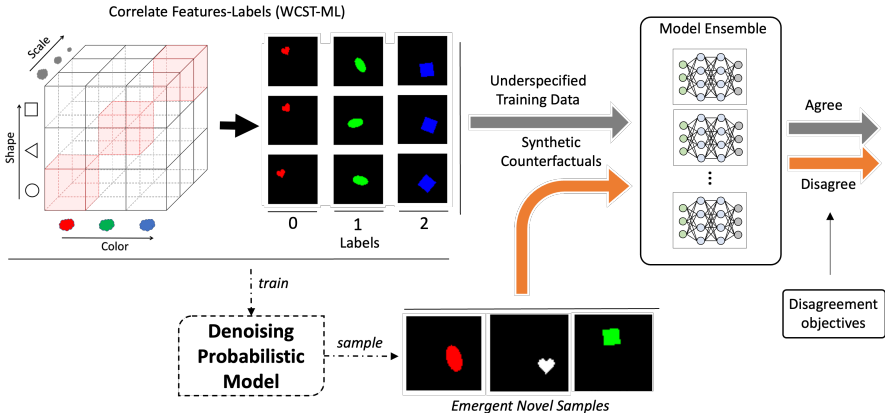


**Fig. 1:** We start with a controlled classification scenario where multiple cues are equally predictive of the target labels, leading to strong simplicity bias tendencies. We consider the WCST-ML setting [28], where the task labels are perfectly correlated with the image input features, e.g. {color, shape, and scale}. We sample from a DPM to generate synthetic counterfactuals showcasing emergent novel feature combinations. Such samples are then utilized for building a diverse model ensemble via different ensemble disagreement objectives.

## 2 Related Work

### 2.1 Overcoming the Simplicity Bias

To overcome the simplicity bias, copious literature has explored methodologies to avoid or mitigate shortcut cue learning when labels for the shortcut cues were present in the training data [8, 10, 12, 14, 25, 35]. The access to shortcut signals is however a critical limitation, as these are generally hard or impossible to obtain. Data augmentation methodologies have proven useful in the generation of *bias-conflicting* or bias-free samples [6, 9, 15], or to augment underrepresented subgroups therein [20, 36], leading to less biased predictions. Although an important research direction, assumptions on the nature of the biases are here still necessary, and the rejection of selected cues for prediction may not always lead to improved generalization, notably when the downstream task is aligned with said cues. A different approach to this problem has instead been to enforce the use of a diverse set of signals for prediction. The use of ensembles has been one such method, where models’ diversity would lead to bias mitigation and improved generalization. Different weight initialization and architectures have previously been shown ineffective in the presence of strong shortcut biases [28]. Methods ensuring mutual orthogonality of the input gradients have proven more

effective, driving models to attend to different locations of the input space for prediction [21, 24, 32, 33]. These input-centric methods, however, may be at a disadvantage in cases where different features must attend to the same area of the input space. Instead, a different approach has been via the diversification of direct ensemble model predictions. This approach hinges on the availability of –unlabelled– out-of-distribution (*ood*) auxiliary samples that are, at least in part, free of the same shortcuts as the original training data. Through a diversification objective, then, the models are made to disagree on these the *ood* samples, effectively fitting functions with different extrapolation behaviors [13, 16, 23, 29]. Even in this case, the auxiliary *ood* data dependency poses limitations, as this is often not readily accessible, and can be costly to procure.

## 2.2 DPMs Modelling and Generalization

In recent years, Diffusion Probabilistic Models have emerged as a transformative generative tool. Numerous studies have underscored their prowess in generating synthetic images, which can then be harnessed to enrich datasets and bolster classification performance [2, 27, 41]. In several cases, DPMs have been shown to transcend the surface-level statistics of the data, making them invaluable in understanding data distributions and features [4, 38, 41]. Moreover, recent studies have indicated the ability of DPMs to achieve feature disentanglement via denoising reconstructions [11, 22, 38]. In particular, work in [37] has shown how text-guided generative models can represent disentangled concepts, and how through algebraic manipulation of their latent representations it is possible to compositionally generalize to novel, and unlikely, image feature combinations. Additional work has also shown strong inductive Diffusion biases during learning, which may explain some of these phenomena [7]. In our work, we test the edge case of DPMs trained with data exhibiting correlated input features. We find that when suitably trained, DPMs can still generate samples with novel feature combinations and that these can be leveraged for ensemble diversity.

## 3 Methods

The following sections describe the experiment pipeline of this paper. In §3.1, as a testbed for our experiments, we introduce an extreme data setup where the task labels are fully correlated with each of the input features. In §3.2, we introduce the datasets considered in our experiments. In §3.3 we then briefly summarize diffusion training and sampling, before presenting the diversification objectives considered in §3.4 and our experimental design in §3.5.

### 3.1 Wisconsin Card Sorting Test for Machine Learners

To isolate and investigate shortcut biases, we employ the Wisconsin Card Sorting Test for Machine Learners (WCST-ML), a method devised to dissect the shortcut learning behaviors of deep neural networks [28]. WCST-ML provides a systematic

approach to creating datasets with multiple cues, designed to correlate with the target labels. Specifically, given  $K$  cues  $i_1, i_2, \dots, i_K$ , the method produces a *diagonal* dataset  $\mathcal{D}_{\text{diag}}$  where each cue  $i_k$  is equally useful for predicting the labels  $Y$ . This level playing field is instrumental in removing the influence of feature dominance and spurious correlations, thereby allowing us to observe a model’s preference for certain cues under controlled conditions. To rigorously test these preferences, WCST-ML employs the notion of *off-diagonal* samples. These are samples where the cues are not in a one-to-one correspondence with the labels, but instead align with only one of the features under inspection. By evaluating a model’s performance on off-diagonal samples, according to each feature, we can test and achieve an estimate of a model’s reliance on the same.

### 3.2 Datasets

As the experimental grounds for our study, we leverage two representative datasets: a color-augmented version of DSprites [18], and UTKFace [43]. The choice of the datasets in our work was due to several factors; most prominently, the *disentangled* nature of the features in DSprites – providing a particularly useful analysis with a controlled overlap of bias tendencies – and a more complex UTKFace, previously known to present strong ethnical bias in WCST-ML training, with concerning societal implications [28].

**DSprites:** DSprites includes a comprehensive set of symbolic objects generated with variations in five latent variables: shape, scale, orientation, and X-Y position. We augment this dataset with a color dimension and remove redundant samples (e.g. due to rotations), resulting in 2,862,824 distinct images, which we refer to as ColorDSprites. ColorDSprites permits the examination of shortcut biases in a highly controlled setup.

**UTKFace:** UTKFace provides a dataset of 23,708 facial images annotated with attributes like age, gender, and ethnicity. Unlike DSprites, UTKFace presents a real-world, less controlled setup to study bias. Its inherent complexity and diversity make it an ideal candidate for understanding the model’s cue preferences when societal and ethical concerns are at stake.

### Operationalizing WCST-ML Across Datasets

We train our models on the correlated WCST-ML diagonal sample sets for both ColorDSprites and UTKFace. For ColorDSprites, we consider  $K_{DS} = 4$ , features  $\{color, orientation, scale, shape\}$ , and  $L = 3$  as constrained by the number of shapes in the dataset. Within UTKFace we consider  $K_{UTK} = 3$ , features  $\{ethnicity, gender, age\}$ , and  $L = 2$  as constrained by the binary classification on *gender*. See §S1 for additional implementation details.

### 3.3 DPMS and Efficient Sampling

We utilize Diffusion Probabilistic Models (DPMS) to generate synthetic data for our experiments. DPMS operate by iteratively adding or removing noise from an

initial data point  $x$  through a stochastic process governed by a predefined noise schedule. Let  $\mathbf{z} = \{\mathbf{z}_t \mid t \in [0, 1]\}$  be a latent variable conditioned on  $t$ , and characterized by a noise-to-signal ratio  $\lambda_t = \log[\alpha_t^2/\sigma_t^2]$  decreasing monotonically with  $t$ . In the forward process, noise is added to  $x$  to transform it into  $z_t$  [26]:

$$q(\mathbf{z}_t \mid \mathbf{x}) = \mathcal{N}(\mathbf{z}_t; \alpha_t \mathbf{x}, \sigma_t^2 \mathbf{I}), \quad q(\mathbf{z}_t \mid \mathbf{z}_s) = \mathcal{N}\left(\mathbf{z}_t; (\alpha_t/\alpha_s) \mathbf{z}_s, \sigma_{t|s}^2 \mathbf{I}\right) \quad (1)$$

where and  $0 \leq s < t \leq 1$ , and  $\sigma_{t|s}^2 = (1 - e^{\lambda_t - \lambda_s}) \sigma_t^2$ . We let  $\alpha_t$  follow a cosine schedules, thus  $\alpha_t = \cos(0.5\pi t)$ .

The reverse process then aims to reconstruct  $x = z_0$  by iteratively denoising  $z_t$  into  $z_s$ , starting from  $z_1 \sim \mathcal{N}(0, I)$ . To facilitate efficient sampling, we employ Denoising Diffusion Implicit Models (DDIM) [31], a first-order ODE solver for DPMs [17, 26], utilizing a predictor-corrector scheme to minimize the number of sampling steps:

$$\begin{aligned} \mathbf{z}_s &= \alpha_s \hat{\mathbf{x}}_\theta(\mathbf{z}_t) + \sigma_s \frac{\mathbf{z}_t - \alpha_t \hat{\mathbf{x}}_\theta(\mathbf{z}_t)}{\sigma_t} \\ &= e^{(\lambda_t - \lambda_s)/2} (\alpha_s/\alpha_t) \mathbf{z}_t + \left(1 - e^{(\lambda_t - \lambda_s)/2}\right) \alpha_s \hat{\mathbf{x}}_\theta(\mathbf{z}_t) \end{aligned} \quad (2)$$

The term  $\hat{\mathbf{x}}_\theta(\mathbf{z}_t)$  is the neural network’s output, predicting the denoised data from the noisy observation at timestep  $t$ . And train the denoising model by:

$$L_\theta = \left(1 + \frac{\alpha_t^2}{\sigma^2}\right) \|\mathbf{x} - \hat{\mathbf{x}}_t\|_2^2 \quad (3)$$

In our setup, we consider DPMs trained at different fidelity levels, postulating that, generally, increased DPM training will more closely fit the data distribution at hand. Therefore, in our experiments, we use the ‘number of diffusion training epochs’ as a proxy for the DPM fidelity on the modeled distribution.

### 3.4 Ensemble Training and Diversification

In our setup, we wish to train a set of models within an ensemble while encouraging model diversity. Let  $f_i$  denote the  $i^{\text{th}}$  model predictions within an ensemble consisting of  $N_m$  models. Each model is trained on a joint objective comprising the conventional cross-entropy loss with the target labels, complemented by a diversification term computed on synthetic counterfactuals, represented as  $L_{\text{div}}$ . The composite training objective is:

$$\mathcal{L} = \mathcal{L}_{\text{xent}} + \gamma \mathcal{L}_{\text{div}}^{\text{obj}} \quad (4)$$

where  $\mathcal{L}_{\text{xent}}$  is the cross-entropy loss,  $\mathcal{L}_{\text{div}}^{\text{obj}}$  is the diversification term for a particular objective, and  $\gamma$  is a hyper-parameter used to modulate the importance of diversification within the optimization objective. To impart diversity to the ensemble, we investigated five diversification objectives denoted by  $obj \in \{\text{div}, \text{cross}, l_1, l_2, \text{kl}\}$ .

We consider the  $l_1$  and  $l_2$  baseline objectives, designed to induce diversity by maximizing the pairwise distance between any two model outputs and the moving average of the ensemble prediction, thus:

$$L_{\text{reg}}^{l_1} = -\frac{1}{N_m} \sum_{i=1}^{N_m} \left\| f_i - \frac{1}{N_m} \sum_{j=1}^{N_m} f_j \right\|_1 \quad (5)$$

$$L_{\text{reg}}^{l_2} = -\frac{1}{N_m} \sum_{i=1}^{N_m} \left\| f_i - \frac{1}{N_m} \sum_{j=1}^{N_m} f_j \right\|_2^2 \quad (6)$$

The *cross* objective diversifies the predictions by minimizing the negative mutual cross-entropy of any two models:

$$\mathcal{L}_{\text{reg}}^{\text{cross}} = -\sum_{i \neq j} \frac{\text{CE}(f_i, \text{argmax}(f_j)) + \text{CE}(f_j, \text{argmax}(f_i))}{2} \quad (7)$$

The *kl* objective aims at maximizing the *kl* divergence between the output distributions of any two models:

$$L_{\text{reg}}^{kl} = -\sum_{i \neq j} D_{KL}(f_i || f_j) \quad (8)$$

Finally, the *div* diversification objective is adapted from [13], and can be summarized as:

$$\mathcal{L}_{\text{reg}}^{\text{div}} = \sum_{i \neq j} D_{KL}(p(f_i, f_j) || p(f_i)) \quad (9)$$

encouraging diversity by minimizing the mutual information of any two models' predictions.

### 3.5 Experiment Design

To investigate the objectives of this study, we apply the WCST-ML framework on ColorDSprites and UTKFace, creating training datasets of fully correlated feature-labels groups (Fig. 1). For ColorDSprites, we consider the features of  $K_{DS} = \{\text{color}, \text{orientation}, \text{scale}, \text{shape}\}$ , while in UTKFace we consider the features  $K_{UTK} = \{\text{ethnicity}, \text{gender}, \text{age}\}$ .

We train two DPMS on the *diagonal* fully-correlated sets of both ColorDSprites and UTKFace, including respectively 34998 and 1634 feature-correlated samples. As mentioned in §3.5, we consider the number of DPM training epochs to be a proxy of the diffusion model's fidelity, or closeness, to the distribution of interest, where longer training generally leads to higher generative consistency of the target distribution. We generate  $\approx 100\text{k}$  samples from DPMS trained at varying number of epochs between 1 to 1K, to be used for ensemble diversification and analysis. We perform no post-processing or pruning of the generated

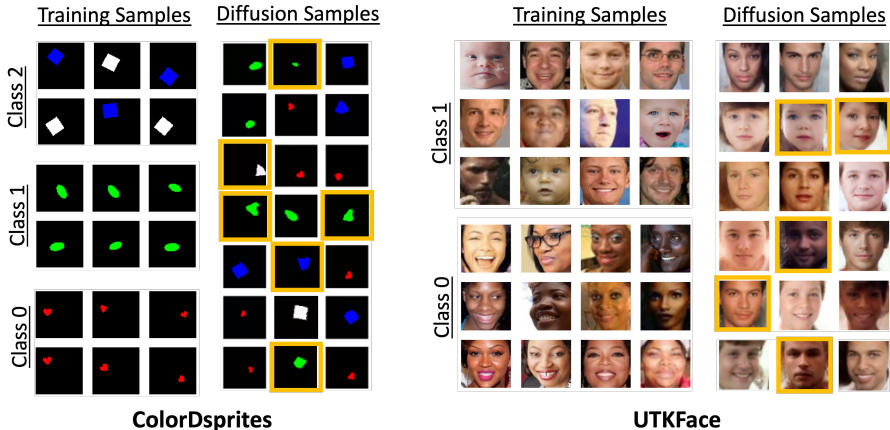


**Fig. 2:** Training and Diffusion Generated samples for ColorDSprites and UTKFace based on WCST-ML. While training on images showcasing a correlated set of features, sampling from DPMs at appropriate fidelity levels can generate novel objects beyond the combinations of features observed during training (marked right-hand side images).

samples, and instead wish to observe the innate ability of DPMs to generate samples beyond the training distribution.

For each of the ensemble experiments, we train a diverse ensemble comprising 100 ResNet-18 models on both ColorDSprites and UTKFace. We perform ensemble training separately with all diversification objectives considered, and for each objective, we perform ablation studies applying the diversification objectives to the data generated by the DPMs at different fidelity levels. For comparison, we also consider ensemble diversification with real *ood* data, randomly sampled from the *off-diagonal* sets, as well as a baseline without a diversification objective.

In summary, the full analysis in this work involved the training of over  $\approx 16,000$  ResNet-18 classifiers (each  $\approx 11$ million parameters), sectioned into 160 ensembles (one for each diffusion-objective pair and baselines), and 31 diffusion models (UNet  $\approx 35$ million parameters).

## 4 Results

### 4.1 Diffusion Disentanglement & ood Sampling

**DPMs Exhibit Generalization Capabilities Under Correlation.** We test the ability of DPMs to transcend surface-level statistics of the data and generate samples that break the shortcut signals at training time, even when trained on correlated data. Fig. 2 displays the training samples for both datasets (left halves), as well as samples from the DPMs (right halves) trained for respectively 25 and 800 epochs. In the figure we observe how sampling from the trained DPMs generates previously unseen feature combinations, despite the correlated

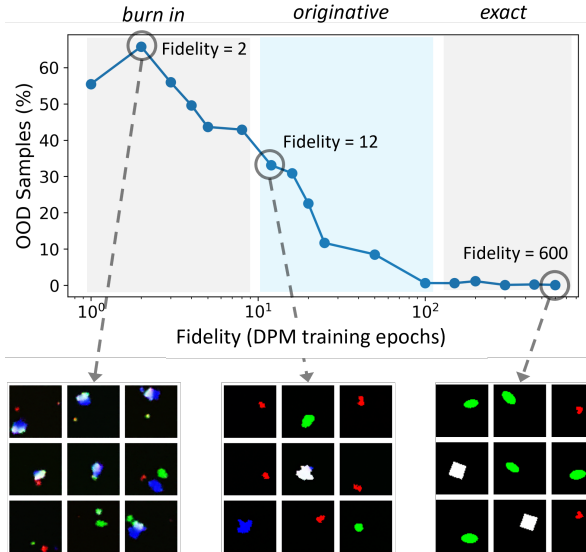


**Fig. 3:** *ood* sample frequency for DPMs trained at different fidelities on ColodDSprites. Three intervals are prominent: *burn-in*, characterized by high *ood* sample frequency, but poor sample quality; *originative*, where the model has learned the manifold of the data while still displaying capabilities for *ood* sample generation; and *exact*, characterized by near-perfect samples, but a significantly reduced *ood* sample generation.

coupling of features during training (e.g.  $\langle \text{green}/\text{white}, \text{heart} \rangle$ ,  $\langle \text{green}, \text{square} \rangle$  or  $\langle \text{child}, \text{female} \rangle$ ), suggesting a potential for innate disentangling capabilities in diffusion latent spaces. Leveraging this powerful capability is crucial in the generation of samples for disagreement, as it allows models to break from the shortcuts in the training distribution.

**Early Stopping to Capture Diffusion *ood* Sampling Capabilities.** To understand under which conditions sampling from DPMs can lead to the generation of samples displaying unseen feature combinations, we examine the fraction of *ood* samples generated by DPMs at different fidelities (§3.5). The ColorDSprites is particularly useful for this analysis, given the disentangled nature of its features. To measure the fraction of *ood* samples, we train a near-perfect oracle on the full ColorDSprites dataset, trained to predict the WCST-ML partitioned labels under all features. We can then consider in-distribution (*id*) those samples showcase fully correlated feature levels (close to the diagonal samples), and out-of-distribution (*ood*) those samples classified to belong to the off-diagonal WCST-ML set. Fig. 3 shows the fraction of *ood* samples generated by the ColorDSprites DPM at varying levels of training fidelities. We identify at least three qualitative different intervals. An initial *burn-in* interval, characterized by a high frequency of *ood* generated samples, but which fails to capture the manifold of the data under inspection; an *originative* interval, where we observe a reduced

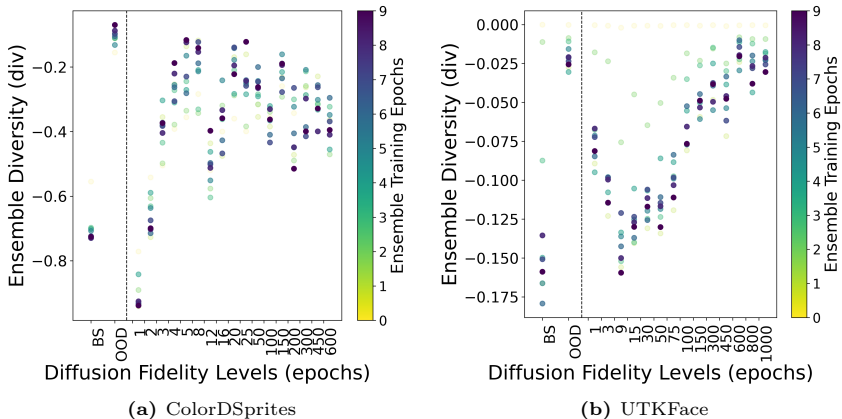


**Fig. 4:** Prediction diversity when diversifying via samples from diffusion models at different fidelities (training epochs), as compared to using real *ood* samples (*ood*), and a baseline without diversification (BS).

number of *ood* samples, in favor for a generative distribution more aligned with the data to represent; and an *exact* interval, where the DPM’s ability to almost perfectly represent the data comes at the cost of novel emergent feature mixtures. In the context of ensemble diversification and bias mitigation, the *originative* interval is posed to provide the necessary information to break the simplicity shortcuts, while providing effective disagreement signals with respect to the visual cues available. We refer the reader to Suppl. §S2 for further insights into DPM-early stopping with ensemble diversification criteria.

## 4.2 Diffusion-guided Ensemble Diversity

We trained a diverse ensemble comprising 100 ResNet-18 models on both ColorDSprites and UTKFace. The ablation studies examined the training of the ensemble with each diversification objective in turn, as well as a baseline with no imposed diversification. For both baseline and diversification experiments, we favor different training dynamics by using separate vanilla Adam optimizers for each model. We train the ensemble with a cross-entropy loss on the correlated diagonal training data, as well as an additional, objective-specific, diversification loss, computed on a separate diversification set. In our experiments, we will refer to ‘*ood*’ when the data for disagreement is comprised of left-out, feature-uncorrelated, samples from the original dataset; to ‘diffusion’ when the samples are generated by a DPM; and to ‘baseline’ when no diversification objective is included. We tune  $\gamma$  by grid-search to provide comparable experiments under different objectives (see Suppl. §S2.1)

**DPM Fidelity Significantly Impacts Diversification.** We consider the case where the diversification objective is computed on samples generated by a DPM

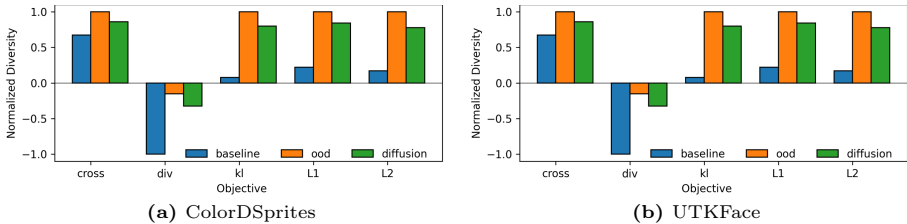


**Fig. 5:** Diversity comparison for ensemble trained on *ood* data and diffusion counterfactuals across metrics (higher is better).

at different fidelity levels. We show in Fig. 4 the diversity achieved on the *div* diversification objective when training the ensemble on the same, with varying diffusion fidelity samples, and report the full set of diversification fidelity experiments in Suppl. Fig S4. In both Fig. 4a and Fig. 4b we observe the diversity of the ensemble predictions to vary significantly, from the low-diversity baseline (BS), trained without a diversification set, to the high diversity achieved with *ood* samples. For both datasets, extremely low fidelities provide little use for diversification, leading to low-diversity predictions by the ensembles. The DPM trained on ColorDSprites, however, quickly fits the synthetic data distribution and provides counterfactual samples achieving similar diversification performance to the original off-diagonal samples at early fidelity levels. Ultimately, excessive diffusion training leads to limited *ood* sample generation and lower diversification performance. The DPM trained on UTKFace trains longer to appropriately model the face data distribution, achieving comparable diversification levels to the *ood* sample set after approximately 800 training epochs. Importantly, these results highlight the benefit of appropriate DPM training and early stopping procedures to generate samples that capture the distribution at hand without displaying over-fit behaviors, affecting the potential to generate novel feature combinations and break the feature shortcuts at training time.

### Diffusion-guided Diversity Leads to Comparably Diverse Ensembles.

Given the difficulty and cost of collecting auxiliary *ood* data for diversification, we wish to compare the level of diversification achieved with DPM counterfactual, as opposed to using real *ood* data. Based on our previous results in Fig. 4 (also Suppl. Fig. S4), we choose early-stopping DPM training at 100 and 800 epochs for ColorDSprites and UTKFace respectively, providing samples especially useful for diversification. In Fig. 5 we report the objective-wise normalized diversity achieved in each scenario by the ensemble. We find that diffusion counterfactuals can lead to comparable diversification performance with respect to real *ood* samples. In the figure, the diffusion-led diversity is almost always within 5% from the metrics achieved when using pure *ood* samples, both typically over 50% higher than the baseline.

**Table 1:** Results on ColorDSprites and UTKFace when using real *ood* samples (upper tables), or diffusion-generated counterfactuals (lower tables), for model disagreement. The feature columns report the fraction of models (not accuracy) biased towards the respective features. The final column reports the average validation accuracy for the ensemble on the left-out feature-correlated *diagonal* set, of the same distribution as the original training data.

### OOD Disagreement

ColorDSprites						UTKFace				
	color	orientation	scale	shape	valid. accuracy (mean +/- std)		age	ethnicity	gender	valid. accuracy (mean +/- std)
<b>baseline</b>	1.00	0.00	0.00	0.00	1.000 +/- 0.00	<b>baseline</b>	0.00	1.00	0.00	0.920 +/- 0.02
<b>cross</b>	0.99	0.00	0.01	0.00	0.865 +/- 0.17	<b>cross</b>	0.01	0.71	0.28	0.865 +/- 0.04
<b>div</b>	0.86	0.01	0.11	0.02	0.818 +/- 0.22	<b>div</b>	0.00	0.94	0.06	0.859 +/- 0.03
<b>kl</b>	0.91	0.02	0.07	0.00	0.822 +/- 0.21	<b>kl</b>	0.05	0.76	0.19	0.818 +/- 0.06
<b>std</b>	0.91	0.00	0.08	0.01	0.813 +/- 0.20	<b>l1</b>	0.02	0.62	0.36	0.847 +/- 0.07
<b>var</b>	0.84	0.02	0.13	0.01	0.729 +/- 0.23	<b>l2</b>	0.03	0.63	0.34	0.798 +/- 0.11

### Diffusion Disagreement

ColorDSprites						UTKFace				
	color	orientation	scale	shape	valid. accuracy (mean +/- std)		age	ethnicity	gender	valid. accuracy (mean +/- std)
<b>baseline</b>	1.00	0.00	0.00	0.00	1.000 +/- 0.00	<b>baseline</b>	0.00	1.00	0.00	0.920 +/- 0.02
<b>cross</b>	0.96	0.00	0.04	0.00	0.856 +/- 0.16	<b>cross</b>	0.00	0.94	0.06	0.836 +/- 0.05
<b>div</b>	0.94	0.00	0.06	0.00	0.916 +/- 0.13	<b>div</b>	0.00	0.98	0.02	0.826 +/- 0.05
<b>kl</b>	0.89	0.01	0.10	0.00	0.786 +/- 0.20	<b>kl</b>	0.00	0.94	0.06	0.837 +/- 0.06
<b>l1</b>	0.89	0.00	0.09	0.02	0.784 +/- 0.20	<b>l1</b>	0.00	0.77	0.23	0.816 +/- 0.11
<b>l2</b>	0.93	0.02	0.03	0.02	0.762 +/- 0.22	<b>l2</b>	0.01	0.83	0.16	0.757 +/- 0.12

**Ensemble Diversification Breaks Simplicity Biases.** By WCST-ML, we can test each model’s bias to a cue by testing the model’s output on purposefully designed test sets [28]. We test the quality of the diversification obtained in Table 1, and ascertained the fraction of models attending to specific cues when trained on out-of-distribution and diffusion-generated samples respectively. A model was deemed to be attending to a cue if its validation accuracy on the cue-specific *ood* WCST-ML dataset was highest relative to all other features. Our baseline findings mirrored the observations in [28]. Specifically, each model in the baseline ensemble predominantly attended the *color* cue in ColorDSprites and the *ethnicity* cue in UTKFace, showcasing strong preferential cue bias while achieving near-perfect classification on diagonal *-id-* validation data. Notably, upon introducing the diversification objectives, we observed a perceptible shift in the models’ behavior, some of which averted their focus from the primary, easy-to-learn cues, turning instead to other latent cues present within the data. Among the objectives considered, *kl*, *l1*, and *l2* exhibited the highest cue diversity, catalyzing the ensemble to distribute attention across multiple cues. However, this also came at the expense of a marked drop in the average ensemble performance. Conversely, the *div* and *cross* objectives yielded milder diversification, focusing

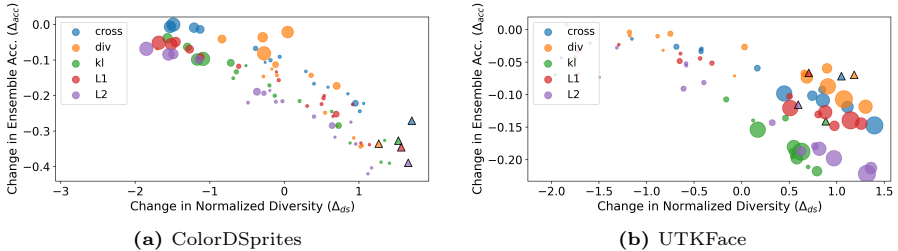


**Fig. 6:** The relationship between the change in normalized classification prediction diversity ( $\Delta_{ds}$ ) and the change in validation accuracy of the ensemble ( $\Delta_{acc}$ ), when trained with samples from DPMs at varying levels of fidelities. The  $\Delta$ s are computed with respect to baseline ensemble training, with no diversification objective. We also compare the metrics achieved by diversification with non-correlated, off-diagonal, *ood* data from the respective datasets.

primarily on the next readily discernible cues, specifically *scale* for ColorDSprites and *gender* for UTKFace, all the while maintaining a generally higher ensemble validation performance. As confirmed in Fig. 5, the diversification achieved by Diffusion counterfactuals in Table 1 is largely comparable with *ood* data on ColorDSprites, with respectively up to 11% and 14% of the models averting their attention from the main ‘color’ cue in ColorDSprites, and up to 23% and 38% of the models averting their attention to the ethnicity cue in UTKFace.

**Increased Ensemble Disagreement Negatively Correlates with Ensemble *id* Performance.** Achieving ensemble diversity by disagreement on unlabelled *ood* samples has previously been shown to negatively impact *id* ensemble performance [23] (suppl. Fig. S1), while improving *ood* performance on downstream tasks associated with non-shortcut cues. Generally, ensemble model selection has been an effective method to prune models that misalign with the original classification objective [13]. In this section, we wish to understand this relationship under the scope of Diffusion-guided diversification. In Fig. 6 we observe the change in ensemble average accuracy  $\Delta_{acc}$  as a function of the change in diversity  $\Delta_{ds}$ , spanning all the diversification objectives. We highlight a few important observations. First, increased ensemble diversity via disagreement negatively correlates with average ensemble accuracy, without additional model selection mechanisms. Second, real *ood* data achieves the highest diversity gain, comparable to the diffusion samples at the *originative* stage (§4.1),  $\approx [10, 100]$  for ColorDSprites, and  $\approx [450, 800]$  for UTKFace. Lastly, the diversification objectives show comparable trends, with the *div* objective displaying marginally better diversification/accuracy performance than the others on both tasks.

## 5 Discussion and Conclusion

Shortcut learning is a phenomenon undermining the performance and utility of deep learning models, where easy-to-learn cues are preferentially learned for

prediction, regardless of their relevance to the downstream task. We investigate the potential of DPMs to aid in the mitigation of this phenomenon by training a diverse ensemble through disagreement on synthetic counterfactuals and show several important findings.

### DPM training and *ood* generation

**Summary.** We show that DPMs can generate novel feature combinations even when trained on images displaying correlated cues. We observe this phenomenon as a function of the diffusion training epochs, suggesting early tendencies of DPMs to learn the manifold of the distribution under scrutiny, without (over)fitting the intricate nuances of the training data.

**Implications and future directions.** Although beyond the scope of this work, it would be worthwhile to understand the mechanism behind the ability of DPMs to generalize beyond the observed feature combinations even under feature correlation. An implication of this finding is the potential of early-stopping mechanisms to enforce these particular generative capabilities. Another significant implication is the potential of DPMs for feature disentanglement and *ood* sample generation, which may have interesting repercussions in several important domains including data augmentation and *ood* generalization.

### Ensemble Diversification

**Summary.** We show that diffusion-guided diversification leads models to avert attention from shortcut cues, and that diffusion counterfactuals can lead to comparable ensemble diversity without the need for expensive *ood* data collection. In our study, we find that there is a delicate balance between the level of diffusion fidelity and the effectiveness of ensemble diversification. In particular, we find that ensemble diversity and validation iid performance can be used as a proxy for the identification of the DPM *originative* stage.

**Limitations and future directions.** We believe it is worthwhile to delve deeper into the interplay between the fidelity of DPM-generated samples and model diversification. A limiting factor in the disagreement objective to achieve shortcut mitigation lies in its impact on average ensemble performance. In prior work, this was partly overcome by careful model selection, but new avenues should be explored to maintain *iid* performance while achieving diverse extrapolation trends via disagreement. Furthermore, although our findings showcase an important phenomenon, and its applicative utility for diverse ensembles, it would also be valuable to extend this work to additional datasets and explore its implications in data modalities beyond vision.

**Conclusion.** This work presents a step forward in addressing the challenge shortcut learning in DNNs. By leveraging the unique capabilities of DPMs for ensemble diversification we provide a practical method that achieves shortcut mitigation in two visual tasks, with only negligible performance loss compared to methods requiring expensive *ood* data collection.

## References

1. Agrawal, A., Batra, D., Parikh, D., Kembhavi, A.: Don't just assume; look and answer: Overcoming priors for visual question answering. In: Proceedings of the IEEE Conference on Computer Vision and Pattern Recognition (CVPR) (June 2018)
2. Azizi, S., Kornblith, S., Saharia, C., Norouzi, M., Fleet, D.J.: Synthetic data from diffusion models improves imagenet classification. arXiv preprint arXiv:2304.08466 (2023)
3. Beery, S., Van Horn, G., Perona, P.: Recognition in terra incognita. In: Proceedings of the European Conference on Computer Vision (ECCV) (September 2018)
4. Chen, Y., Viégas, F., Wattenberg, M.: Beyond surface statistics: Scene representations in a latent diffusion model. arXiv preprint arXiv:2306.05720 (2023)
5. Geirhos, R., Jacobsen, J.H., Michaelis, C., Zemel, R., Brendel, W., Bethge, M., Wichmann, F.A.: Shortcut learning in deep neural networks. *Nature Machine Intelligence* **2**(11), 665–673 (Nov 2020). <https://doi.org/10.1038/s42256-020-00257-z>, <https://doi.org/10.1038/s42256-020-00257-z>
6. Jung, Y., Shim, H., Yang, J.Y., Yang, E.: Fighting fire with fire: contrastive debiasing without bias-free data via generative bias-transformation. In: International Conference on Machine Learning. pp. 15435–15450. PMLR (2023)
7. Kadkhodaie, Z., Guth, F., Simoncelli, E.P., Mallat, S.: Generalization in diffusion models arises from geometry-adaptive harmonic representation. arXiv preprint arXiv:2310.02557 (2023)
8. Kim, B., Kim, H., Kim, K., Kim, S., Kim, J.: Learning not to learn: Training deep neural networks with biased data. In: 2019 IEEE/CVF Conference on Computer Vision and Pattern Recognition (CVPR). pp. 9004–9012. IEEE Computer Society, Los Alamitos, CA, USA (jun 2019). <https://doi.org/10.1109/CVPR.2019.00922>, <https://doi.ieeecomputersociety.org/10.1109/CVPR.2019.00922>
9. Kim, E., Lee, J., Choo, J.: Biaswap: Removing dataset bias with bias-tailored swapping augmentation. In: Proceedings of the IEEE/CVF International Conference on Computer Vision. pp. 14992–15001 (2021)
10. Kirichenko, P., Izmailov, P., Wilson, A.G.: Last layer re-training is sufficient for robustness to spurious correlations. In: The Eleventh International Conference on Learning Representations (2023), <https://openreview.net/forum?id=Zb6c8A-Fghk>
11. Kwon, M., Jeong, J., Uh, Y.: Diffusion models already have a semantic latent space. arXiv preprint arXiv:2210.10960 (2022)
12. Lee, J., Kim, E., Lee, J., Lee, J., Choo, J.: Learning debiased representation via disentangled feature augmentation. *Advances in Neural Information Processing Systems* **34**, 25123–25133 (2021)
13. Lee, Y., Yao, H., Finn, C.: Diversify and disambiguate: Learning from underspecified data. arXiv preprint arXiv:2202.03418 (2022)
14. Li, Y., Vasconcelos, N.: Repair: Removing representation bias by dataset re-sampling. In: 2019 IEEE/CVF Conference on Computer Vision and Pattern Recognition (CVPR). pp. 9564–9573. IEEE Computer Society, Los Alamitos, CA, USA (jun 2019). <https://doi.org/10.1109/CVPR.2019.00980>, <https://doi.ieeecomputersociety.org/10.1109/CVPR.2019.00980>
15. Lim, J., Kim, Y., Kim, B., Ahn, C., Shin, J., Yang, E., Han, S.: Biasadv: Bias-adversarial augmentation for model debiasing. In: Proceedings of the IEEE/CVF Conference on Computer Vision and Pattern Recognition. pp. 3832–3841 (2023)

16. Lin, Y., Tan, L., Hao, Y., Wong, H., Dong, H., Zhang, W., Yang, Y., Zhang, T.: Spurious feature diversification improves out-of-distribution generalization. arXiv preprint arXiv:2309.17230 (2023)
17. Lu, C., Zhou, Y., Bao, F., Chen, J., Li, C., Zhu, J.: Dpm-solver: A fast ode solver for diffusion probabilistic model sampling in around 10 steps. *Advances in Neural Information Processing Systems* **35**, 5775–5787 (2022)
18. Matthey, L., Higgins, I., Hassabis, D., Lerchner, A.: dsprites: Disentanglement testing sprites dataset. <https://github.com/deepmind/dsprites-dataset/> (2017)
19. Minderer, M., Bachem, O., Houlsby, N., Tschannen, M.: Automatic shortcut removal for self-supervised representation learning. In: *Proceedings of the 37th International Conference on Machine Learning. ICML'20, JMLR.org* (2020)
20. Mondal, A.K., Singhal, L., Tiwary, P., Singla, P., Prathosh, A.: Minority over-sampling for imbalanced data via class-preserving regularized auto-encoders. In: *International Conference on Artificial Intelligence and Statistics*. pp. 3440–3465. PMLR (2023)
21. Nicolicioiu, A.M., Nicolicioiu, A.L., Alexe, B., Teney, D.: Learning diverse features in vision transformers for improved generalization. arXiv preprint arXiv:2308.16274 (2023)
22. Okawa, M., Lubana, E.S., Dick, R.P., Tanaka, H.: Compositional abilities emerge multiplicatively: Exploring diffusion models on a synthetic task. arXiv preprint arXiv:2310.09336 (2023)
23. Pagliardini, M., Jaggi, M., Fleuret, F., Karimireddy, S.P.: Agree to disagree: Diversity through disagreement for better transferability. arXiv preprint arXiv:2202.04414 (2022)
24. Ross, A., Pan, W., Celi, L., Doshi-Velez, F.: Ensembles of locally independent prediction models. In: *AAAI* (2020)
25. Sagawa\*, S., Koh\*, P.W., Hashimoto, T.B., Liang, P.: Distributionally robust neural networks. In: *International Conference on Learning Representations* (2020), <https://openreview.net/forum?id=ryxGuJrFvS>
26. Salimans, T., Ho, J.: Progressive distillation for fast sampling of diffusion models. arXiv preprint arXiv:2202.00512 (2022)
27. Sariyildiz, M.B., Alahari, K., Larlus, D., Kalantidis, Y.: Fake it till you make it: Learning transferable representations from synthetic imagenet clones. In: *CVPR 2023–IEEE/CVF Conference on Computer Vision and Pattern Recognition* (2023)
28. Scimeca, L., Oh, S.J., Chun, S., Poli, M., Yun, S.: Which shortcut cues will dnns choose? a study from the parameter-space perspective. In: *International Conference on Learning Representations* (2022)
29. Scimeca, L., Rubinstein, A., Nicolicioiu, A., Teney, D., Bengio, Y.: Leveraging diffusion disentangled representations to mitigate shortcuts in underspecified visual tasks. In: *NeurIPS 2023 Workshop on Diffusion Models* (2023), <https://openreview.net/forum?id=AvUAVYRA70>
30. Shah, H., Tamuly, K., Raghunathan, A., Jain, P., Netrapalli, P.: The pitfalls of simplicity bias in neural networks. In: *Proceedings of the 34th International Conference on Neural Information Processing Systems. NIPS'20, Curran Associates Inc., Red Hook, NY, USA* (2020)
31. Song, J., Meng, C., Ermon, S.: Denoising diffusion implicit models. arXiv preprint arXiv:2010.02502 (2020)
32. Teney, D., Abbasnejad, E., Lucey, S., van den Hengel, A.: Evading the simplicity bias: Training a diverse set of models discovers solutions with superior OOD generalization. In: *CVPR* (2022)

33. Teney, D., Peyrard, M., Abbasnejad, E.: Predicting is not understanding: Recognizing and addressing underspecification in machine learning. arXiv preprint arXiv:2207.02598 (2022)
34. Torralba, A., Efros, A.A.: Unbiased look at dataset bias. In: CVPR 2011. pp. 1521–1528 (2011). <https://doi.org/10.1109/CVPR.2011.5995347>
35. Wang, T., Zhao, J., Yatskar, M., Chang, K., Ordonez, V.: Balanced datasets are not enough: Estimating and mitigating gender bias in deep image representations. In: 2019 IEEE/CVF International Conference on Computer Vision (ICCV). pp. 5309–5318. IEEE Computer Society, Los Alamitos, CA, USA (nov 2019). <https://doi.org/10.1109/ICCV.2019.00541>, <https://doi.ieeecomputersociety.org/10.1109/ICCV.2019.00541>
36. Wang, X., Lyu, Y., Jing, L.: Deep generative model for robust imbalance classification. In: Proceedings of the IEEE/CVF Conference on Computer Vision and Pattern Recognition. pp. 14124–14133 (2020)
37. Wang, Z., Gui, L., Negrea, J., Veitch, V.: Concept algebra for (score-based) text-controlled generative models. In: Thirty-seventh Conference on Neural Information Processing Systems (2023)
38. Wu, Q., Liu, Y., Zhao, H., Kale, A., Bui, T., Yu, T., Lin, Z., Zhang, Y., Chang, S.: Uncovering the disentanglement capability in text-to-image diffusion models. In: Proceedings of the IEEE/CVF Conference on Computer Vision and Pattern Recognition. pp. 1900–1910 (2023)
39. Xiao, K.Y., Engstrom, L., Ilyas, A., Madry, A.: Noise or signal: The role of image backgrounds in object recognition. In: International Conference on Learning Representations (2021), <https://openreview.net/forum?id=gl3D-xY7wLq>
40. Xu, T., White, J., Kalkan, S., Gunes, H.: Investigating bias and fairness in facial expression recognition. In: Computer Vision – ECCV 2020 Workshops: Glasgow, UK, August 23–28, 2020, Proceedings, Part VI. p. 506–523. Springer-Verlag, Berlin, Heidelberg (2020). [https://doi.org/10.1007/978-3-030-65414-6\\_35](https://doi.org/10.1007/978-3-030-65414-6_35), [https://doi.org/10.1007/978-3-030-65414-6\\_35](https://doi.org/10.1007/978-3-030-65414-6_35)
41. Yuan, J., Pinto, F., Davies, A., Gupta, A., Torr, P.: Not just pretty pictures: Text-to-image generators enable interpretable interventions for robust representations. arXiv preprint arXiv:2212.11237 (2022)
42. Zech, J.R., Badgeley, M.A., Liu, M., Costa, A.B., Titano, J.J., Oermann, E.K.: Variable generalization performance of a deep learning model to detect pneumonia in chest radiographs: A cross-sectional study. *PLoS Med.* **15**(11), e1002683 (Nov 2018)
43. Zhang, Z., Song, Y., Qi, H.: Age progression/regression by conditional adversarial autoencoder. In: Proceedings of the IEEE conference on computer vision and pattern recognition. pp. 5810–5818 (2017)

## S1 Supplementary Methods

### S1.1 Operationalizing WCST-ML Across Datasets

We follow the set-up in [28] and construct a balanced dataset  $\mathcal{D}_{\text{diag}}$ , which includes a balanced distribution of cues, coupled with their corresponding off-diagonal test sets (one for each feature). For both datasets, we define a balanced number of classes  $L$  for each feature under investigation. Where the number of feature values exceeds  $L$ , we dynamically choose ranges to maintain sample balance with respect to each new feature class. For instance, for the continuous feature ‘age’ in UTKFace, we dynamically select age intervals to ensure the same  $L$  number of categories as other classes, as well as sample balance within each category. We consider sets of features previously found to lead to strong simplicity biases. For ColorDSprites, we consider  $K_{DS} = 4$ , features  $\{color, orientation, scale, shape\}$ , and  $L = 3$  as constrained by the number of shapes in the dataset. Within UTKFace we consider  $K_{UTK} = 3$ , features  $\{ethnicity, gender, age\}$ , and  $L = 2$  as constrained by the binary classification on *gender*. For each dataset we create one *diagonal* subset of fully correlated features and labels, available at training time, and  $K_{DS}$  and  $K_{UTK}$  feature-specific *off-diagonal* datasets to serve for testing the models’ shortcut bias tendencies.

## S2 Supplementary Results

### S2.1 $\gamma$ Selection

We perform a hyper-parameter search to find the values of  $\gamma$  for each diversification objective. We perform the search via the same methodology used in the *ood* main experiments, i.e. by training an ensemble of 100 ResNet-18 models on the fully correlated *diagonal* datasets, while diversifying a small subset of 30% of the original training data, randomly sampled from the de-correlated left-out set. We consider  $\gamma$  values ranging from  $1e-3$  to  $1e1$ , and monitor both the validation ensemble accuracy as well as the predictive diversity on a separate de-correlated set of validation data. Figure S1 shows the performance of each metric for different values of  $\gamma$ . We select the values reported in Table S1 to be at the intersection of the accuracy and diversification trends for each model.

### S2.2 On the Influence of DPM Fidelity to Diversification

We perform experiments whereby an ensemble of 100 ResNet-18 models is trained separately with respect to all diversification objectives considered. Figure S4 shows the diversification results as a function of the fidelity of the DPM used to sample the diversification set. We observe the diversification level obtained is highly dependent on the diffusion fidelity level, and that appropriate early stopping procedures are necessary to achieve increased ensemble prediction diversity. While the trends vary mildly across different disagreement objectives, we find the diversification maximized in ColorDSprites and UTKFace coherently with

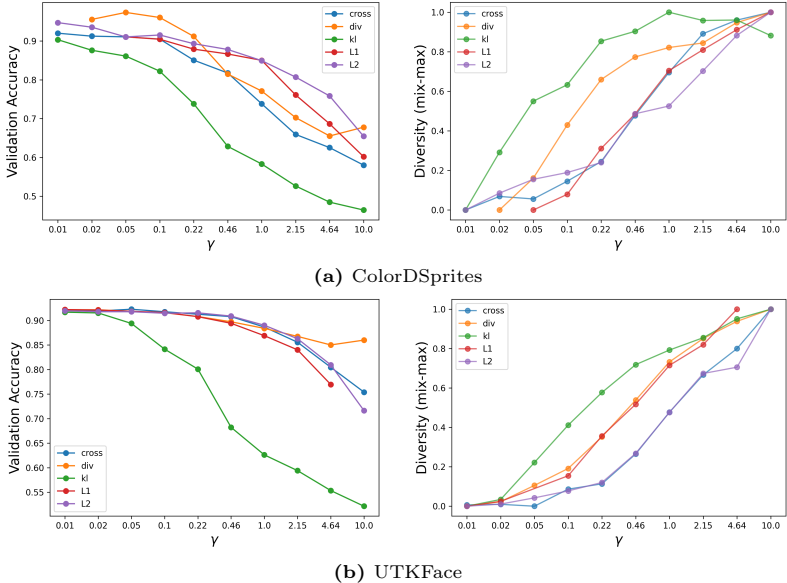


**Fig. S1:** Hyper-parameter search on the disagreement intensity ( $\gamma$ ) for each diversification objective. For the main experiments, we select the values of  $\gamma$ s at the intersection of the accuracy-diversity trends by each objective (Table S1).

**Table S1:** Disagreement  $\gamma$  used in our experiments.

	12	12	cross	div	kl
<b>color</b>	5.0	1.5	0.5	0.5	0.1
<b>face</b>	5.0	2.0	2.0	5.0	0.2

the analysis in Section 4.1, where improved diversification is achieved around the *originative* interval. For ColorDSprites, this is realized in around 20 DPM training epochs, while for UTKFace, it is realized in around 800 DPM training epochs.

Importantly, our results suggest how ensemble diversification metrics can be a viable proxy for appropriate *originative* DPM training. In Fig. S3, we observe the min-maxed change in accuracy and change in diversity by the ensembles with respect to baseline training. In the figure, we observe similar trends across all diversification methods, whereby the *originative* interval (highlighted in gray) identified by the highest changes in diversity and least drop in accuracy, highly overlaps with our previous supervised findings (Fig. 3). Our results align with our previous observations, where the highest number of ood-generated samples to lie within the DPM training intervals achieve the highest change in diversity while maintaining good classification performance (Fig. 6.)

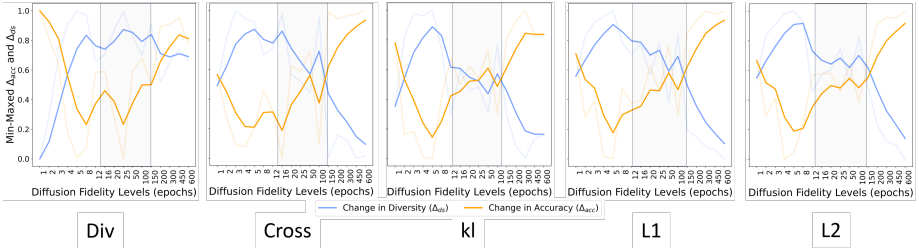


Fig. S2: ColorDSprites

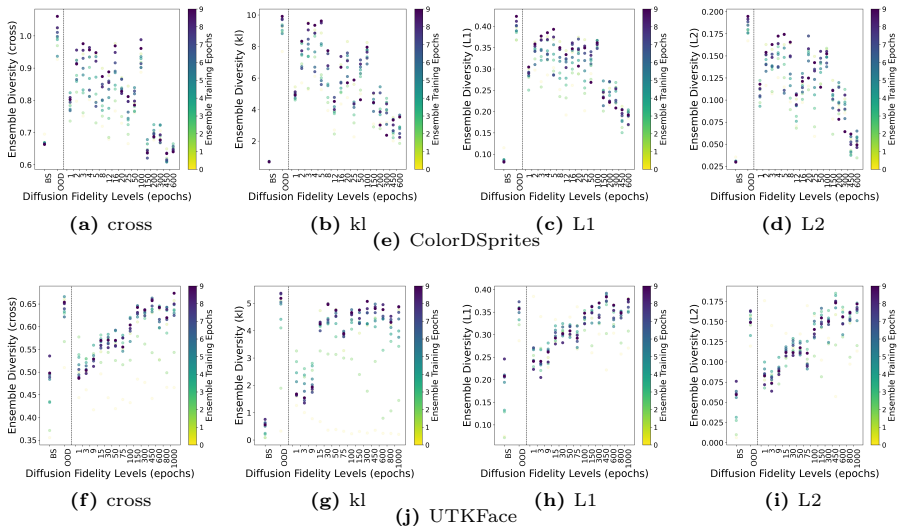
**Fig. S3:** Min-Maxed change in accuracy and diversity by ensembles trained with diffusion-augmented samples, with respect to all considered diversification methods. The *originitive* stage, as qualitatively identified in the experiments (see Fig. 3 and Fig. 4) is shown in gray.

### S2.3 Diversification Leads to Ensemble Models Attending to Different Cues

Figure S5 illustrates a feature-centric description of 10 ensemble models trained with a diversification objective on *ood* data (a) and Diffusion generated counterfactuals (b). Within each results are shown for ColorDSprites (upper panel) and UTKFace (lower panel). The variation across models is evident: several models substantially reduce their dependency on the leading cues of the respective datasets (black edges), diverging considerably from the almost identical configurations present in the baseline ensemble (red edges). For some of the models, the averted attention on the main shortcut cue leads to increased reliance on one of the other observed features (e.g. scale and age for models 7 (above) and 73 (below) in Fig. S5a, and models 80 (above) and 47 (below) in Fig. S5b). In some, however, the averted attention on the main shortcut cues instead leads to a reliance on extracted image features unobserved in our experiments (e.g. Models 28 (above) and 67 (below) in Fig. S5a, and models 98 (above) and 48 (below) in Fig. S5b)).

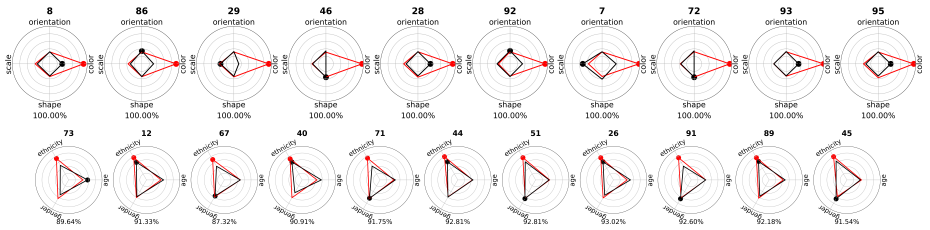
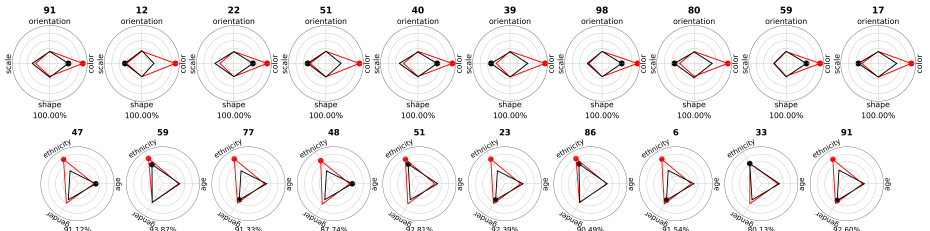
### S2.4 On the Influence of an Increased Number of *ood* Samples for Ensemble Disagreement

As per the original objective, with DPM sampling we aim to circumvent the diversification dependency on Out-Of-Distribution data, which is often not readily accessible and can be costly to procure. We test this dependency further and assess the quality of the diversification results when matching the number of *ood* data used for diversification to the original training data for the ensemble. We report in Table S2 our findings. We observe the quality of the disagreement on ColorDSprites to only marginally benefit from additional disagreement samples, with approximately 1% to 7% more of the models to avert their attention from the shortcut cue *color* as compared to the original experiments. On the



**Fig. S4:** Ensemble diversity as enforced via samples from diffusion models trained a different fidelity levels (i.e. diffusion training epochs).

other hand, we observe a strong improvement in the diversification for UTK-Face, mainly registered via the *div* objective, where 24% of the models averted their attention from the *ethnicity* shortcut, as opposed to the original 6% in our previous experiments, while maintaining high predictive performance on the validation set. We observe marginal improvements on the other objectives, with approximately 4% to 8% additional models achieving cue aversion. We speculate this gain to be due to the higher complexity of the features within the data, which may require additional specimens for appropriate diversification.

(a) *ood* Disagreement

(b) Diffusion Disagreement

**Fig. S5:** Comparison of 10 diversified models when training the ensemble while using (a) feature-uncorrelated *ood* data and (b) Diffusion Samples.

**Table S2:** Diversification results on ColorDSprites and UTKFace when using the same number of *ood* samples as the training dataset. The feature columns report the fraction of models (in each row) biased towards the feature. The final column reports the average validation accuracy for the ensemble when tested on a left-out feature-correlated *diagonal* set, of the same distribution as the original training data

ColorDSprites

	color	orientation	scale	shape	valid. accuracy (mean +/- std)
<b>baseline</b>	1.00	0.00	0.00	0.00	1.000 +/- 0.00
<b>cross</b>	0.92	0.00	0.08	0.00	0.849 +/- 0.16
<b>div</b>	0.82	0.00	0.18	0.00	0.820 +/- 0.19
<b>kl</b>	0.90	0.03	0.05	0.02	0.801 +/- 0.20
<b>l1</b>	0.90	0.01	0.07	0.02	0.799 +/- 0.21
<b>l2</b>	0.86	0.04	0.08	0.02	0.745 +/- 0.22

UTKFace

	age	ethnicity	gender	valid. accuracy (mean +/- std)
<b>baseline</b>	0.00	1.00	0.00	0.920 +/- 0.02
<b>cross</b>	0.00	0.73	0.27	0.858 +/- 0.04
<b>div</b>	0.00	0.76	0.24	0.844 +/- 0.04
<b>kl</b>	0.02	0.68	0.30	0.820 +/- 0.07
<b>l1</b>	0.00	0.66	0.34	0.832 +/- 0.09
<b>l2</b>	0.08	0.58	0.34	0.761 +/- 0.15